THE JOURNAL OF BIOLOGICAL CHEMISTRY VOL. 282, NO. 40, pp. 29414–29423, October 5, 2007

Cytoskeletal Anchoring of GLAST Determines Susceptibility to Brain Damage

*AN IDENTIFIED ROLE FOR GFAP**

Received for publication, May 21, 2007, and in revised form, August 1, 2007 Published, JBC Papers in Press, August 6, 2007, DOI 10.1074/jbc.M704152200

Susan M. Sullivan[‡1], Aven Lee[§], S. Tracey Björkman[¶], Stephanie M. Miller[¶], Robert K. P. Sullivan[‡], Philip Poronnik[§], Paul B. Colditz[¶], and David V. Pow[‡2]

From the [‡]School of Biomedical Sciences, University of Newcastle, Callaghan, New South Wales 2308, Australia, [§]School of Biomedical Sciences, University of Queensland, St. Lucia, Queensland 4072, Australia, and [¶]Perinatal Research Centre, University of Queensland, Royal Brisbane and Women's Hospital, Herston, Queensland 4029, Australia

Glial fibrillary acidic protein (GFAP) is an enigmatic protein; it currently has no unambiguously defined role. It is expressed in the cytoskeleton of astrocytes in the mammalian brain. We have used co-immunoprecipitation to identify *in vivo* binding partners for GFAP in the rat and pig brain. We demonstrate interactions between GFAP, the glutamate transporter GLAST, the PDZ-binding protein NHERF1, and ezrin. These interactions are physiologically relevant; we demonstrate *in vitro* that transport of D-aspartate (a glutamate analogue) is significantly increased in the presence of GFAP and NHERF1. Moreover, we demonstrate *in vivo* that expression of GFAP is essential in retaining GLAST in the plasma membranes of astrocytes after an hypoxic insult. These data indicate that the cytoskeleton of the astrocyte plays an important role in protecting the brain against glutamate-mediated excitotoxicity.

Glial fibrillary acidic protein (GFAP)[3] is an intermediate filament protein that is expressed by subsets of white and gray matter astrocytes in the central nervous system (1, 2). Intriguingly, specific functions have not been ascribed for GFAP, despite, for instance, evidence for increased GFAP mRNA in Alzheimer disease and Creutzfeldt-Jacob disease and decreased GFAP levels in Down syndrome (2).

Mutations in the GFAP gene are believed to cause a fatal condition, Alexander disease. However, it is not known how expression of the mutant GFAP protein leads to brain damage (3).

Analyses of brains from GFAP knock-out mice suggest that glutamate transport activity is reduced (4). The plasmalemmal glutamate transporters, including GLAST and GLT-1, which are expressed by astrocytes in the brain, normally act to maintain low extracellular levels of glutamate (5–7). Glutamate has the potential to act as a potent excitotoxin when present at high concentrations or for long periods in the extracellular space, causing excessive activation of ionotropic glutamate receptors; thus it is a major contributing factor in hypoxia-related brain injury (8–12). Because GFAP is expressed by astrocytes and because it appears to influence glutamate transport capacity, we hypothesized that glutamate transporters might be linked to the astrocyte cytoskeleton.

Hypoxia is a major cause of brain damage, especially in neonates, much of which is mediated by glutamate excitotoxicity (13, 14). We have previously shown that hypoxic insults cause region-specific damage to the neonatal pig brain and that the patterns of cellular damage are in precise topographical register with the patterns of loss of GLAST (15). There is currently no known reason why astrocytes in some brain regions would lose their glutamate transporters whereas others do not.

In this study, we examined the potential relationship between GFAP and GLAST using multiple methods. We have used co-immunoprecipitation to identify potential binding partners of GFAP in the brain and transfection studies to characterize the functional consequences of interactions on transport activity. Finally, we have examined the topographic co-expression of these proteins in the hypoxically insulted brain.

EXPERIMENTAL PROCEDURES

All animal experiments were carried out in accordance with National Health and Medical Research Council (Australia) guidelines and the Queensland Protection of Animals Act. This legislation accords with and exceeds the ethical requirements of National Institutes of Health guidelines. All studies were approved by the University of Queensland or University of Newcastle Animal Ethics Committees. Sprague-Dawley rats were obtained from the University of Newcastle or University of Queensland animal breeding facilities. Male and female piglets (Landrace X Large White) were obtained from The University of Queensland piggeries on the day of birth. For ethical reasons, all hypoxia experiments were performed on anesthetized animals; thereafter, the animals were allowed to recover consciousness.

Antibodies—The GLAST, GLT-1α, and GLT-1b antibodies used in this study have been extensively characterized in previous studies, including pig (15, 16). Mouse monoclonal anti-GFAP antibody was purchased from Sigma or Chemicon (Temecula, CA). Mouse monoclonal anti-ezrin was purchased from Invitrogen. A rabbit polyclonal antibody against the C-terminal region of NHERF1 (a gift from Dr. C. Yun) was used

* This work was supported by National Health and Medical Research Council (NH&MRC) (Australia) project grants. The costs of publication of this article were defrayed in part by the payment of page charges. This article must therefore be hereby marked "*advertisement*" in accordance with 18 U.S.C. Section 1734 solely to indicate this fact.
[1] Supported by an Australian Postgraduate Award scholarship.
[2] Supported by an NH&MRC Senior Research fellowship and a Gladys Brawn Senior Research fellowship. To whom correspondence should be addressed. Tel.: 61249215620; Fax: 61249218667; E-mail: d.pow@eaats.org.
[3] The abbreviations used are: GFAP, glial fibrillary acidic protein; PBS, phosphate-buffered saline; shRNA, short hairpin RNA; IP, immunoprecipitation.

as previously described (17). Monoclonal anti-green fluorescent protein antibody was purchased from BD Biosciences.

Lysate Preparation—Brain tissues were isolated from rats or pigs that had been euthanized by an overdose of sodium pentobarbital (100 mg/kg, intraperitoneally). Rat brain tissues were homogenized in immunoprecipitation lysis buffer containing phosphate-buffered saline (PBS) (137 mM NaCl, 2.7 mM KCl, 1.5 mM KH_2PO_4, 7.7 mM Na_2HPO_4, pH 7.4), 1% Triton X-100, and protease inhibitor mixture (Roche Diagnostics). Pig brain tissues were homogenized in immunoprecipitation (IP) lysis buffer containing 50 mM Tris-HCl, pH 8.0, 150 mM NaCl, 1% Nonidet P-40, and protease inhibitor mixture (Roche Diagnostics). After gentle rotation for 3 h at 4 °C, homogenates were centrifuged at 100,000 × *g* for 1 h at 4 °C and the supernatant collected.

GFAP Immunoprecipitation in Rat Brain—Brain lysates were precleared with protein G-agarose (Roche Diagnostics) for 3 h at 4 °C and incubated with anti-GFAP or IgG overnight at 4 °C. Protein G-agarose beads were added and the samples incubated at 4 °C for 3 h. The protein G-agarose was then gently washed five times in IP lysis buffer. SDS sample buffer was added to the pellet and heated to 95 °C for 5 min. Proteins were separated on a 7% SDS-PAGE gel and stained with Coomassie blue to visualize all potential binding partners of GFAP.

Rat Brain Co-immunoprecipitation and Immunoblotting—Rat brain co-immunoprecipitation experiments were performed using the Profound Mammalian Co-immunoprecipitation kit (Pierce Biotechnology Inc.) following the manufacturer's instructions. Antibodies (against GLAST, GLT-1α, GLT-1b, NHERF1, ezrin, or GFAP) were covalently immobilized to an AminoLink® coupling gel that was subsequently packed onto a spin column. Rabbit/mouse IgG was used as a control. Rat brain total lysate was subjected to the column and incubated with gentle mixing overnight at 4 °C to allow binding of the antigen to the immobilized antibody. After several wash steps with IP lysis buffer, the immunoprecipitated complex was eluted from the column by addition of ImmunoPure IgG elution buffer and directly resolved on a 7% SDS-PAGE gel. The proteins were transferred to a nitrocellulose membrane (Bio-Rad Laboratories) by electroblotting and incubated with appropriate antibodies (against GLAST, GLT-1α, GLT-1b, NHERF1, ezrin, or GFAP) overnight at 4 °C in 5% nonfat milk, 100 mM Tris, pH 7.5, 306 mM NaCl, and 0.1% Tween 20. The membrane was washed four times with Tris-NaCl-Tween buffer, incubated for 1 h with horseradish peroxidase-conjugated anti-rabbit/mouse IgG (Pierce), and washed again. Immunoreactive proteins were detected by enhanced chemiluminescence using the SuperSignal® West Dura Extended Duration Substrate kit (Pierce).

Pig Brain Co-immunoprecipitation and Immunoblotting—Pig brain lysates were precleared with Protein G-agarose (Roche Diagnostics) for 3 h at 4 °C and incubated with anti-GFAP or a non-relevant antibody control (anti-green fluorescent protein) overnight at 4 °C. Protein G-agarose beads were added and the samples incubated at 4 °C for 3 h. The protein G-agarose was then gently washed five times in IP lysis buffer. SDS sample buffer was added to the pellet and heated to 95 °C for 5 min. Immunoblotting for pig brain samples was performed as for the rat brain samples described above.

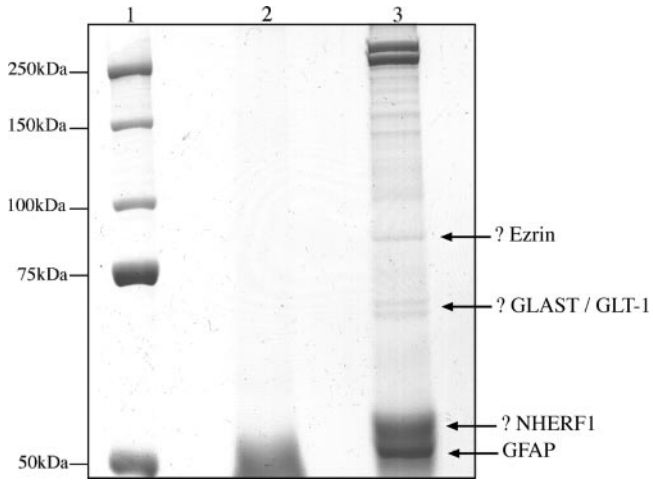

FIGURE 1. **Coomassie-stained gel of GFAP immunoprecipitation products in rat brain.** *Lane one*, molecular mass marker; *lane 2*, IgG control; *lane 3*, rat GFAP immunoprecipitation product. Many proteins associate with GFAP in the rat brain, as shown by bands of varying intensities and a range of molecular masses. GFAP has at least ten *in vivo* binding partners between 50–300 kDa. The positions of bands that potentially correspond to binding partners NHERF1, GLAST/GLT-1, and ezrin are indicated.

Cell Culture and Transfection—293FT packaging cells (Invitrogen) were grown and maintained in high glucose Dulbecco's modified Eagle's medium supplemented with 10% fetal bovine serum, 0.1 mM non-essential amino acids, 6 mM L-glutamine, and 500 μg/ml Geneticin in a 5% CO_2 environment. COS7 cells were grown and maintained in high glucose Dulbecco's modified Eagle's medium containing 10% fetal bovine serum in a 5% CO_2 environment. For D-aspartate uptake studies, COS7 cells were plated in 12-well dishes. At 70–80% confluency, the cells were co-transfected with pcDNA3.1 (control) or pcDNA3.1:GFAP (a kind gift from Dr. Michael Brenner, University of Alabama) plus either pGLAST or pGLASTΔpdz by using Lipofectamine LTX (Invitrogen). The transfected COS7 cells were cultured for 3–4 days before performing D-aspartate uptake assays (described below). pGLASTΔpdz was a GLAST C-terminal deletion mutant without the PDZ binding motif (ETKM) and was generated using the QuikChange site-directed mutagenesis kit (Stratagene) from the wild-type pGLAST construct. The effective transfection and high level of expression were verified by Western blot analysis.

Lentivirus Production and Infection of COS7 Cells—The shRNA Constructs (TRCN0000068583, TRCN0000068584, TRCN0000068585, TRCN0000068586, and TRCN-0000068587) for NHERF1 knock down were obtained from The RNAi Consortium via Open Biosystems (Huntsville, AL). Five pre-made constructs were obtained and tested to identify those able to achieve efficient knock down at the protein level. The negative control construct in the same vector system (vector alone) was also obtained from The RNAi Consortium via Open Biosystems. The lentiviral packaging plasmid psPAX2 and envelope plasmid pMD2G were obtained from Dr. Didier Trono (School of Life Sciences, Lausanne, Switzerland). To prepare virus stocks, 293FT cells were co-transfected with shRNA constructs, together with psPAX2 and pMD2G constructs (4:3:1 ratio, respectively), using Lipofectamine 2000 (Invitrogen). The medium was changed after

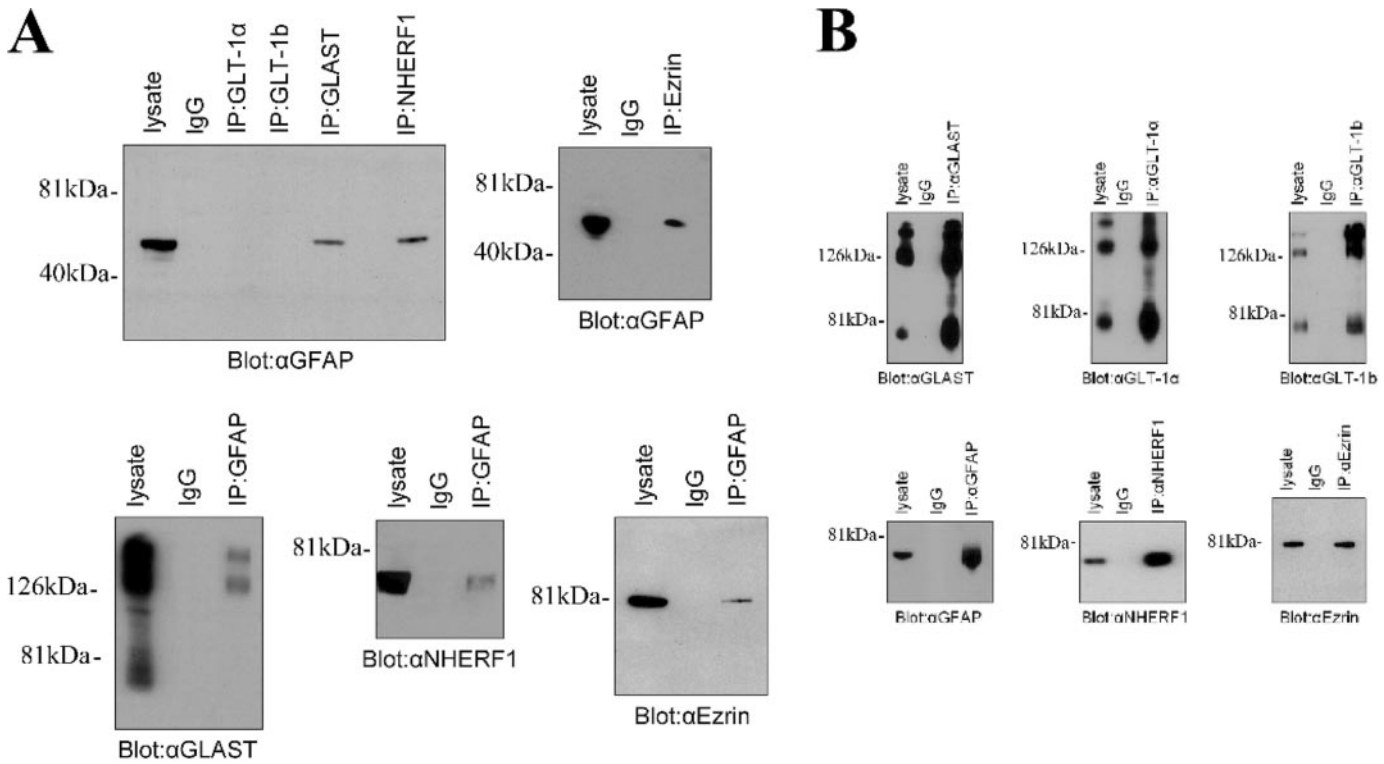

FIGURE 2. **Co-immunoprecipitation of GLAST, NHERF1, ezrin, and GFAP in rat brain.** Antibodies (against GLAST, GLT-1α, GLT-1b, NHERF1, ezrin, or GFAP) were coupled to an AminoLink® Plus Gel (see "Experimental Procedures") and incubated with total rat brain lysate. The immunoprecipitated products (*IP*) were resolved by SDS-PAGE and immunoblotted with appropriate antibodies (as indicated). *A*, immunoblots of the IP show that GLAST, NHERF1, and ezrin co-precipitate with GFAP and vice versa. *B*, immunoblots showing that the target proteins were immunoprecipitated.

24 h, and virus-containing medium was collected after 36–48 h. The viral stocks were centrifuged and filtered through a 0.45-μm filter to remove any nonadherent 293FT cells. Cultures of COS7 cells or transfected COS7 cells were infected with a mixture of 0.5 ml of shRNA lentivirus-containing medium and 0.5 ml of regular medium. The medium was changed 24 h post-infection and replaced with regular Dulbecco's modified Eagle's medium.

D-Aspartate Uptake Assays—COS7 cells were washed twice with transport buffer containing 140 mM NaCl, 5 mM KCl, 2 mM $CaCl_2$, 2 mM $MgCl_2$, 10 mM HEPES, pH 7.5, and 4.5 g/liter of glucose. COS7 cells were then incubated in transport buffer containing [^{3}H]D-aspartate (Amersham Biosciences) and 5 μM unlabeled D-aspartate for 10 min at 25 °C. Cells were washed three times with ice-cold transport buffer in which NaCl was replaced by choline chloride and solubilized with lysis buffer containing 20 mM Hepes-Tris, pH 7.5, 120 mM NaCl, 1% Triton X-100, 5 mM EDTA. Aliquots were taken for scintillation counting, protein assays, and Western blot analysis. The radioactivity counts were adjusted according to the protein content of the sample and expressed as nmol D-aspartate/mg of protein/min.

COS7 Cell Co-immunoprecipitation and Immunoblotting—Co-immunoprecipitation of interacting proteins from transfected COS7 cells was carried out using the ProFound Mammalian Co-immunoprecipitation kit (Pierce). Anti-GLAST antibody was covalently immobilized to an AminoLink® antibody-coupling gel. COS7 cells in T25-cm^2 flasks (at 70–80% confluency) were transiently co-transfected with pcDNA3.1 (control) or pcDNA3.1:GFAP plus either pGLAST or pGLASTΔpdz by

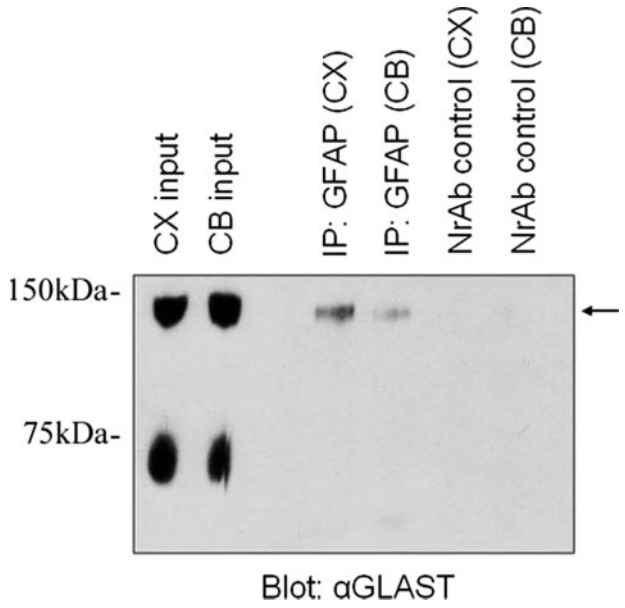

FIGURE 3. **Co-immunoprecipitation of GFAP and GLAST in pig cortex and cerebellum.** Total lysate prepared from pig cortex (*CX*) and cerebellum (*CB*) were incubated with anti-GFAP or a non-relevant antibody control (*NrAb*; anti-green fluorescent protein) and precipitated using protein G beads. The samples were resolved by SDS-PAGE and immunoblotted with anti-GLAST antibodies. Native monomeric and dimeric forms of GLAST were detected in the lysate-input samples (~65 and ~130 kDa; *lanes 1* and *2*). A band was detected at ~130 kDa (*arrow*) representing the dimeric form of GLAST in products immunoprecipitated with anti-GFAP antibodies (*lanes 3* and *4*). This band was not detected in products immunoprecipitated with the non-relevant antibody control (*NrAb*) (*lanes 5* and *6*).

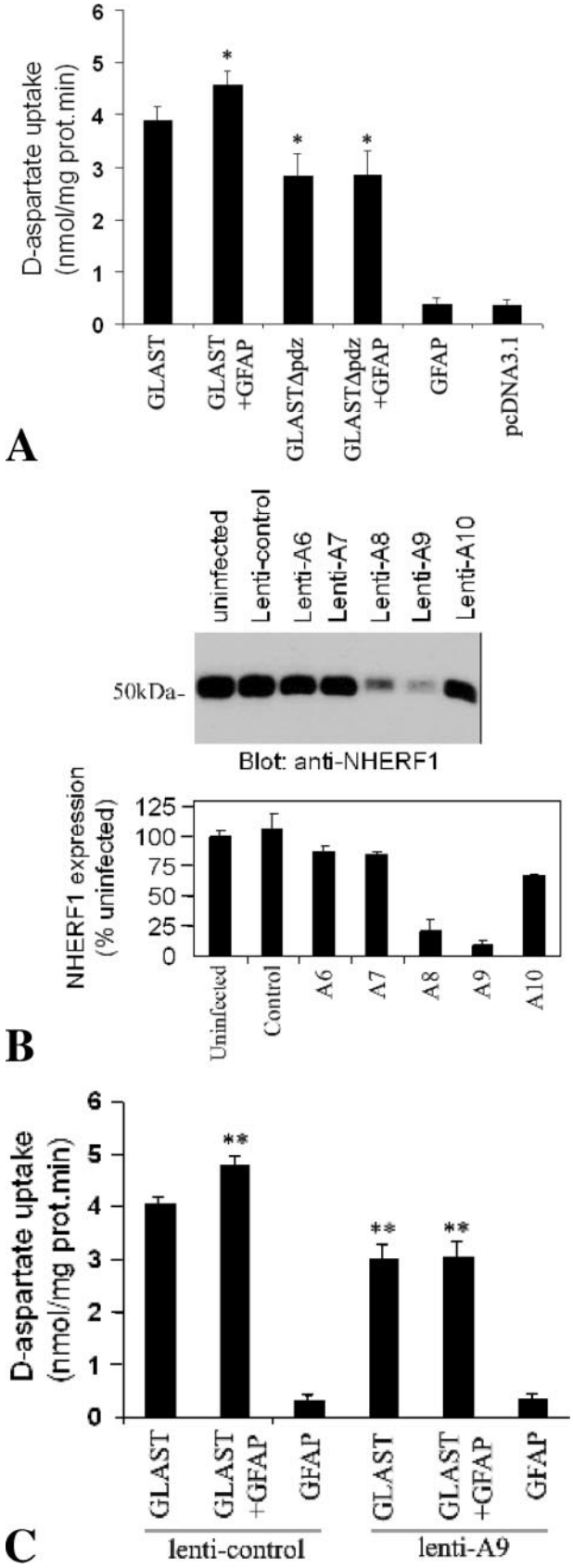

FIGURE 4. **Modulation of GLAST transport activity by GFAP involves PDZ-mediated interactions.** *A*, effect of co-expression of GLAST or GLASTΔpdz with GFAP on D-aspartate uptake in COS7 cells. Co-expression of GLAST and GFAP caused a significant increase in the amount of transported D-aspartate compared with expression of GLAST alone ($p < 0.05$). Expression of GLASTΔpdz with or without GFAP significantly reduced D-aspartate uptake compared with wild-type GLAST expression ($p < 0.05$), indicating the importance of the PDZ binding motif in functional transport by GLAST and interaction with GFAP. *Bars* indicate S.D. of the mean; *asterisks* indicate statistical significance ($p < 0.05$) *versus* control (COS7 cells expressing GLAST only). *B*, knock down of endogenous NHERF1 by lentiviral shRNAs. Following infection with various lentiviral shRNAs (as indicated), expression of endogenous NHERF1 in whole cell lysate was analyzed by Western blotting. Greatest knock down of endogenous NHERF1 was seen with Lenti-A9 (>90%). Each lane was loaded with 20 μg of total lysate. *C*, effect of NHERF1 knock down on GLAST-GFAP-mediated D-aspartate uptake in COS7 cells. Transfected COS7 cells were infected with either lentiviral shRNA (*lenti-A9*) targeted for NHERF1 gene or a non-target control lentiviral shRNA (*lenti-control*). Knock down of NHERF1 by lenti-A9 significantly decreased D-aspartate uptake in GLAST- and GLAST-GFAP-expressing COS7 cells when compared with lenti-control treatment. *Bars* indicate S.D. of the mean; *double asterisks* indicate statistical significance ($p < 0.01$) *versus* control (lenti-control-infected COS7 cells expressing GLAST only).

using Lipofectamine LTX (Invitrogen). Three to four days after transfection, cells were rinsed with ice-cold PBS and harvested in lysis buffer containing PBS and 1% Triton X-100 supplemented with protease inhibitor mixture (Roche). After lysis for 30 min at 4 °C, lysates were clarified by centrifugation for 20 min at 30,000 × *g* at 4 °C. For NHERF1 knockdown experiments, transfected cells were infected with a mixture of 2 ml of shRNA lentivirus-containing medium and 2 ml of regular medium. The medium was changed 24 h post-infection and replaced with regular Dulbecco's modified Eagle's medium and further incubated for 4–5 days before lysis as described above. Precleared lysate was applied to the antibody-coupled gel and incubated overnight at 4 °C with gentle end-to-end rotation. The protein-antibody-coupled gel was washed with lysis buffer, and protein complexes were eluted in ImmunoPure elution buffer, boiled in sample buffer, and resolved by SDS-PAGE. Proteins were transferred to nitrocellulose membrane and immunoblotted with anti-GFAP as described above.

Quantification of Results and Statistical Analysis—Data from three independent uptake experiments (performed in triplicate) were analyzed and presented as mean value ± S.D. Statistical significances were estimated using one-way analysis of variance with Dunnet's test (Graph Pad Prism v4.0). Western blot data from NHERF1 knockdown experiments (performed in triplicate) were analyzed using Scion Image (Scion Corp.). A significance level threshold of $p = 0.05$ was used in this study.

Immunocytochemical Experiments—Sprague-Dawley rats ($n = 6$) were euthanized by an overdose of sodium pentobarbital (120 mg/kg, intraperitoneally). Animals were fixed initially by perfusion via the heart with 4% paraformaldehyde in 0.1 M sodium phosphate buffer (PBS, pH 7.2). Anesthetized neonatal piglets ($n = 6$) were rendered hypoxic by exposure to 4% oxygen for 30 min and monitored as previously described in detail (18). Littermate controls ($n = 6$) underwent anesthesia only and were then allowed to recover for 72 h. At the completion of each experiment, pigs were euthanized with an overdose of sodium pentobarbital (120 mg/kg, intraperitoneally).

Tissue Preparation for Immunocytochemistry—Rat brains were removed after perfusion-fixation and fixed by immersion for an additional 1 h in 4% paraformaldehyde plus 10% picric acid in PBS. Pig brain tissues were removed and 3-mm-thick slices prepared using a brain slice matrix. Slices were fixed by immersion in 4% paraformaldehyde plus 10% picric acid for

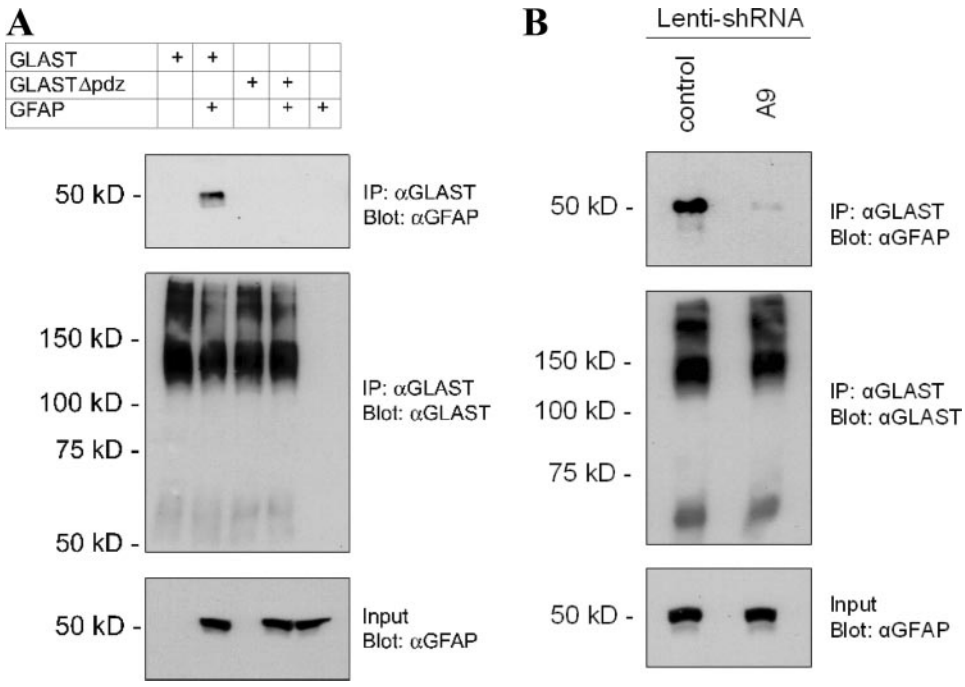

FIGURE 5. **Co-immunoprecipitation of GFAP and GLAST in transfected COS7 cells.** *A*, constructs encoding GLAST, GLASTΔpdz, or GFAP were co-transfected in COS7 cells as indicated, and lysates were immunoprecipitated with anti-GLAST antibodies followed by immunoblot analysis with anti-GFAP antibodies. Immunoprecipitation (*IP*) analysis showed that wild-type GLAST, but not GLASTΔpdz, interacted with GFAP. For each experiment, control blots were performed to confirm the expression of the constructs in the transfected COS7 cell lysates. *B*, COS7 cells co-expressing GLAST and GFAP were infected with either lentiviral shRNA (*A9*) targeted for NHERF1 gene or a non-target (*control*) lentiviral shRNA. Total lysate was collected 4–5 days later and immunoprecipitated with anti-GLAST antibodies followed by immunoblot analysis with anti-GFAP antibodies. IP analysis showed that knock down of NHERF1 impaired the GFAP-GLAST interaction. For each experiment, control blots were performed to confirm the expression of the constructs in the COS7 cell lysates.

12 h. All brains were then processed for paraffin wax embedding according to standard protocols (15).

Immunocytochemistry and Microscopy—Serial coronal sections of paraffin wax-embedded brains (8 μm in thickness) were cut on a rotary microtome and mounted onto silanated microscope slides. Sections were dewaxed with xylene and then rehydrated through a graded series of ethanol/water mixtures. Antigen recovery was performed using Revealit-Ag antigen recovery solution (ImmunoSolution, NSW, Australia).

Immunocytochemical labeling was performed for GFAP (1:3,000) or GLAST (1:5,000) using standard immunoperoxidase methods with species-specific secondary antibodies (Amersham Biosciences) followed by streptavidin-horseradish peroxidase complex (Amersham Biosciences); labeling was revealed using 3,3′-diaminobenzidine as a chromogen. Sections were viewed with an Olympus BX51 microscope equipped with an Olympus DP70 digital camera. Low magnification images of entire brain hemisections were scanned using a Nikon Coolscan IV slide scanner.

Dual immunolabeling for GLAST (1:1,000) and GFAP (1:500) was performed using species-specific secondary antibodies labeled with Texas Red (for GLAST) or fluorescein isothiocyanate (for GFAP). Confocal imaging was performed using a Nikon C1 confocal microscope equipped with solid state lasers emitting at 488 and 594 nm to excite fluorescein isothiocyanate and Texas Red, respectively.

Digital images were imported into Adobe Photoshop 7. Only minor contrast and brightness adjustments were made. Composite plate images of the digital files were generated using Macromedia Freehand X.

RESULTS

GFAP Binding Partners—Total rat brain lysate was immunoprecipitated with the GFAP antibody; the products were separated by SDS-PAGE and stained with Coomassie blue to initially evaluate whether a significant number of proteins were associated with GFAP *in vivo*. Multiple potential binding partners for GFAP were detected (represented by bands of differing intensities), including at least ten proteins with molecular masses between 50 and 300 kDa (Fig. 1). We noted in particular two bands at ~65 kDa and one at ~80 kDa. These were selected for further investigation because they corresponded to predicted molecular masses of the known glial markers GLAST, GLT-1, and ezrin. The band at ~50 kDa includes GFAP. However, the broad nature of this band indicated the probable presence of other proteins of a similar molecular mass, such as NHERF1 (~52 kDa).

In Vivo Interaction between GFAP and GLAST in Rat Brain—We next asked whether the glutamate transporters GLAST, GLT-1α, or GLT-1b co-associate with GFAP in rat brain. We used polyclonal antibodies to immunoprecipitate GLAST, GLT-1α, and GLT-1b from brain lysate, and the recovered immunocomplexes were subjected to immunoblot analysis. As GLAST was recently shown to associate with the PDZ scaffold protein NHERF1 and the microfilament membrane linker ezrin (17), we also included NHERF1- and ezrin-immunoprecipitated products in our analysis. Immunoprecipitates obtained using anti-GLAST, anti-NHERF1, and anti-ezrin antibodies (but not anti-GLT-1α and anti-GLT-1b) contained GFAP, represented by the band detected at ~50 kDa (Fig. 2*A*). To further confirm the interactions, we immunoprecipitated total rat brain lysate with monoclonal anti-GFAP antibody and detected GLAST (Fig. 2*A*); the bands detected at ~130 and ~195 kDa represented the dimeric and trimeric forms of GLAST, respectively (19). The immunoprecipitated complex obtained using anti-GFAP also contained NHERF1 and ezrin, represented by the bands detected at ~52 and ~80 kDa, respectively (Fig. 2*A*), but not GLT-1α or GLT-1b (data not shown). Western blots showing that the target proteins were immunoprecipitated are shown in Fig. 2*B*. Taken together, these results would indicate that in brain, GLAST, NHERF1, and ezrin associate with GFAP.

In Vivo Interaction between GFAP and GLAST in Pig Brain—To determine whether the GLAST-GFAP interaction described above in rat was relevant and replicable in other

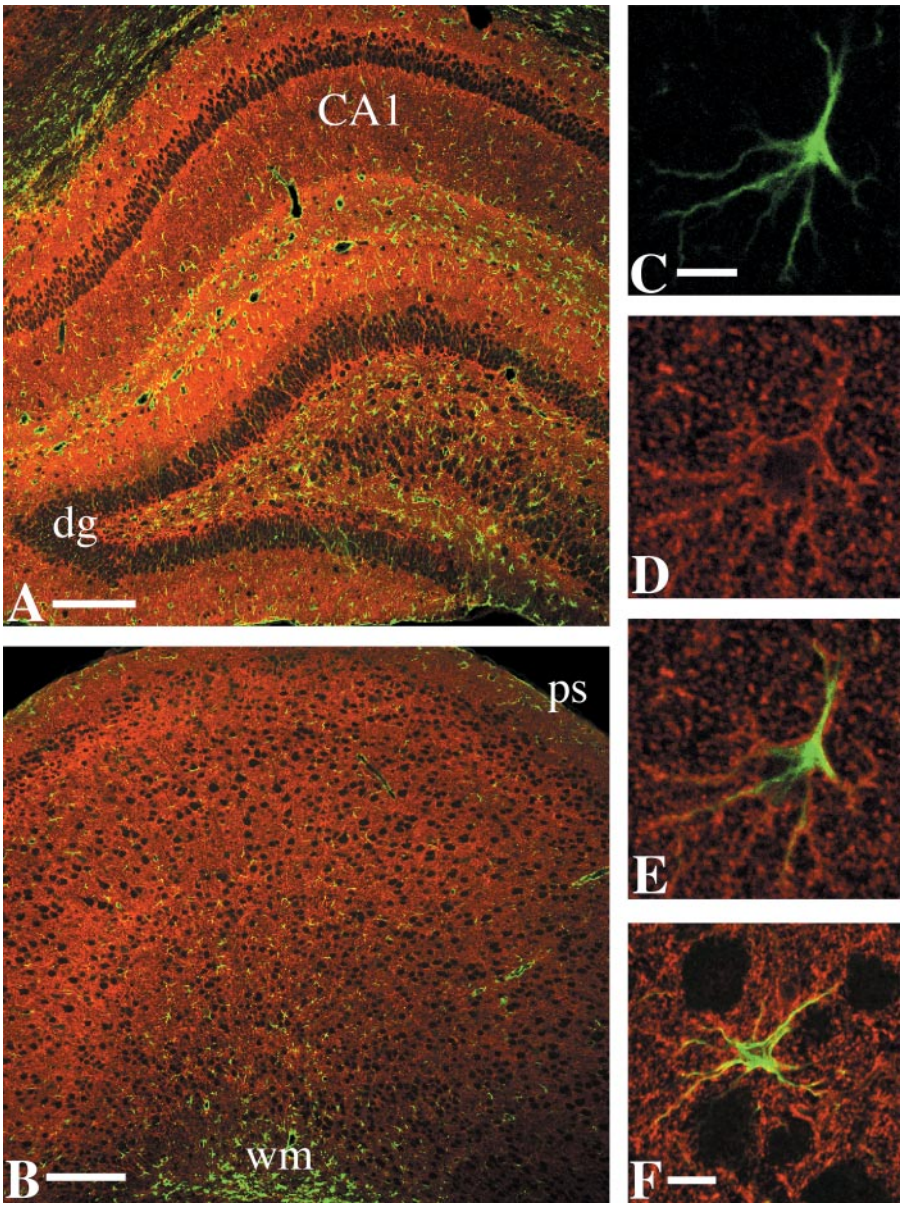

FIGURE 6. **Dual immunofluorescence labeling of rat brain for GFAP (*green*) and GLAST (*red*).** GFAP was expressed in gray matter astrocytes and highly expressed in white matter astrocytes (*wm*). GLAST was widely expressed in gray matter, including hippocampus (*A*) and cortex (*B*). *C–E*, individual astrocyte from the hippocampus showing labeling for GFAP (*C*), GLAST (*D*), and merged image (*E*). GLAST was expressed in the plasma membrane of this GFAP-labeled astrocyte. *F*, co-expression of GFAP and GLAST in a single gray matter astrocyte. *dg*, dentate gyrus. *Scale bars*, *A* and *B*, 100 μm; *C–F*, 10 μm.

mammalian species, the immunoprecipitation experiments were also performed using pig brain lysate. We immunoprecipitated total pig brain lysate with monoclonal anti-GFAP antibodies, and the recovered immunocomplexes were subjected to immunoblot analysis. As shown in Fig. 3, the immunocomplexes obtained using anti-GFAP antibodies contained GLAST, with the band detected at ~130 kDa representing the dimeric form of GLAST. Immunoprecipitation with a non-relevant antibody control (monoclonal anti-green fluorescent protein) did not immunoprecipitate GLAST (Fig. 3). GFAP immunoprecipitation complexes were also blotted with anti-GLT-1α and anti-GLT-1b antibodies; however, no association was detected between GFAP and GLT-1 (data not shown). We further confirmed the GLAST-GFAP interaction by immunoprecipitating total brain lysate with an anti-GLAST antibody and detected GFAP (data not shown).

Modulation of GLAST Transport by GFAP Involves PDZ-mediated Interactions—To assess whether GFAP could modulate GLAST-mediated transport, we performed [^{3}H]D-aspartate uptake assays in COS7 cells co-expressing GFAP and wild-type GLAST or a GLAST C-terminal PDZ motif deletion mutant (GLASTΔpdz). Expression of wild-type GLAST alone in COS7 cells resulted in a ~12-fold increase in D-aspartate uptake over mock-transfected cells. Co-expression of wild-type GLAST and GFAP resulted in a significant increase (~17%) in D-aspartate uptake compared with wild-type GLAST alone (Fig. 4*A*). COS7 cells expressing GLASTΔpdz alone had a significant reduction (~27%) in D-aspartate uptake compared with wild-type GLAST (Fig. 4*A*). Furthermore, co-expression of GLASTΔpdz and GFAP in COS7 cells did not increase D-aspartate uptake above that of GLASTΔpdz alone (Fig. 4*A*).

To assess the role of NHERF1 in the GFAP-GLAST interaction, we used lenti-shRNA to knock down endogenous NHERF1 in COS7 cells. Initially, several lenti-shRNAs were generated against the mouse NHERF1 sequence and tested on COS7 cells. Lenti-A9 specifically reduced endogenous NHERF1 protein expression by >90% (Fig. 4*B*) but did not affect NHERF2 expression (data not shown). COS7 cells expressing wild-type GLAST alone or in combination with GFAP were then infected with lenti-A9 to assess the role of NHERF1 in GLAST/GLAST-GFAP-mediated D-aspartate uptake. D-Aspartate uptake was significantly reduced (~26%) in lenti-A9-treated COS7 cells expressing wild-type GLAST compared with cells infected with control lentivirus (Fig. 4*C*). Treatment with lenti-A9 also abolished the GFAP-stimulated component of D-aspartate transport in COS7 cells co-expressing GLAST and GFAP (Fig. 4*C*).

We further tested the interaction between GLAST/GLASTΔpdz and GFAP in transfected COS7 cells by co-immunoprecipitation. Constructs encoding GLAST, GLASTΔpdz, and GFAP were transfected in COS7 cells, and cell lysates were immunoprecipitated with anti-GLAST antibodies followed by immunoblot analysis. As shown in Fig. 5*A*, GFAP was found to

co-precipitate with wild-type GLAST but not with the PDZ deletion mutant, GLASTΔpdz. As negative controls, GFAP was not detected in anti-GLAST immunoprecipitations from cells transfected with only GLAST, GLASTΔpdz, or GFAP. We also showed that the GFAP-GLAST interaction was greatly impaired when endogenous NHERF1 was knocked down (Fig. 5*B*). Taken together, the results suggested that the GFAP-GLAST interaction was dependent on the GLAST C-terminal PDZ binding motif (ETKM) and association with NHERF1.

Immunofluorescence Labeling for GFAP and GLAST in the Rat Brain—Because the co-immunoprecipitation data suggested GFAP can form a complex *in vivo* that included GLAST, immunolabeling was used to further examine the relationship between the two proteins in the rat brain. GFAP expression was modest and widespread in gray matter astrocytes and highly expressed in white matter astrocytes. The glutamate transporter GLAST was abundantly expressed in gray matter astrocytes throughout the rat brain, including hippocampus and cortex (Fig. 6, *A* and *B*). High magnification confocal images revealed a co-association of GFAP and GLAST in gray matter astrocytes. GFAP was expressed in the core of the astrocyte process, whereas GLAST was expressed in the plasma membranes of the astrocytes (Fig. 6, *C–F*).

GFAP and GLAST Expression in Normal Pig Brain—Analysis of normal pig brain tissues revealed that GFAP was also expressed by astrocytes in gray and white matter of pig brain (Fig. 7*A*). Similarly, analysis of serial sections immunolabeled for GLAST revealed high expression in the gray matter of the cortex, in hippocampus, and in other forebrain regions such as thalamus and hypothalamus (Fig. 7*B*).

GFAP and GLAST Expression in Hypoxic Pig Brain—Comparison of the patterns of labeling for GFAP (Fig. 7, *C* and *E*) and GLAST (Fig. 7, *D* and *F*) in hypoxic brains, obtained on serial sections, revealed a remarkable level of coincidence at the macroscopic level. GFAP expression was up-regulated in the gray matter in those areas such as the dentate gyrus where the GLAST expression was retained, whereas in areas where GLAST expression was lost (such as the CA1 region of the hippocampus) GFAP expression was minimal.

Significant loss of GLAST was evident in areas such as the cortex, particularly layers 2–5, and subregions of the hippocampus such as the CA1 region. Conversely, some areas such as the dentate gyrus of the hippocampus usually exhibited little, if any, evidence for damage (Fig. 7, *D* and *F*, *arrows*). Damage in other brain regions was also heterogeneous; thus only subregions of the thalami appeared to have lost expression of GLAST.

To determine whether GFAP co-localized with GLAST in normal or hypoxic pig tissues, dual immunofluorescence labeling was performed. Expression patterns of both proteins were compared with results obtained for single-labeled sections (Fig. 8, *A–C*). After hypoxic insults, little expression of either GFAP or GLAST was observed in the CA1 hippocampal region. Conversely, GFAP and GLAST were highly expressed and co-localized in the adjacent dentate gyrus. High magnification confocal images revealed that GFAP and GLAST were co-associated in a subset of gray matter astrocytes in the control pig brain as they were in the rat brain, with GFAP expressed in the core or

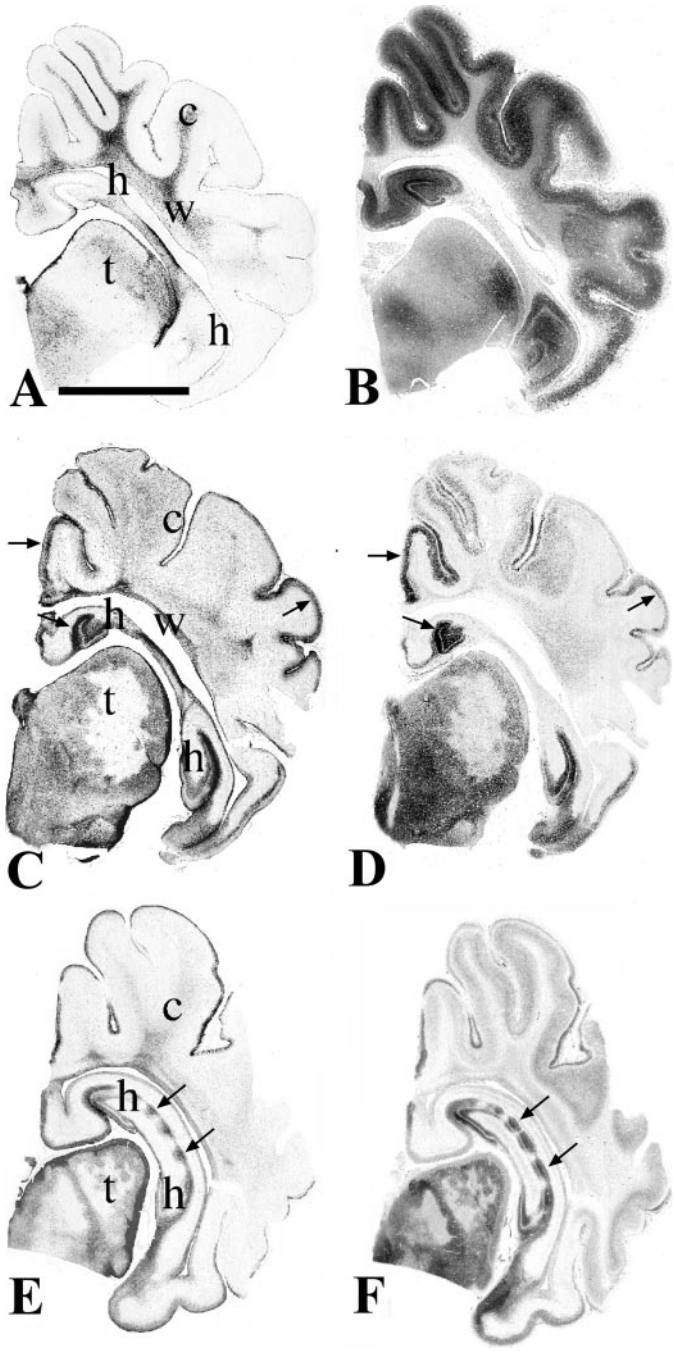

FIGURE 7. **Coronal hemisections of normal (*A*, *B*) and hypoxic brains (*C*, *D* and *E*, *F*), labeled for GFAP (*A*, *C*, *E*) and GLAST (*B*, *D*, *F*).** In normal brain, GFAP labeling was strongest in white matter areas (*w*). In hypoxic animals (*C*, *E*), GFAP was up-regulated in gray matter of specific brain regions, including dentate gyrus of hippocampus (*h*, *arrows*), some regions of thalamus (*t*), and in the outer layers of some parts of cortex (*c*, *arrows*). In normal animals, GLAST (*B*) was extensively expressed in gray matter areas. In hypoxic animals, there was extensive loss of GLAST expression in some areas, including the CA1 region (*D*, *F*). Conversely, GLAST expression remained high in areas of gray matter such as dentate gyrus (*arrows*, *D*). Areas of gray matter that retained expression of GLAST also expressed increased levels of GFAP (*C–F*, *arrows*). *Scale bar*, 1 cm.

cytoskeleton of the astrocyte and GLAST expressed in the plasma membrane (Fig. 8, *D–F*).

The association of these two proteins was most striking in hypoxic tissues. In some areas of cortex from hypoxic brains, GLAST expression was retained in the outer layers of cortex,

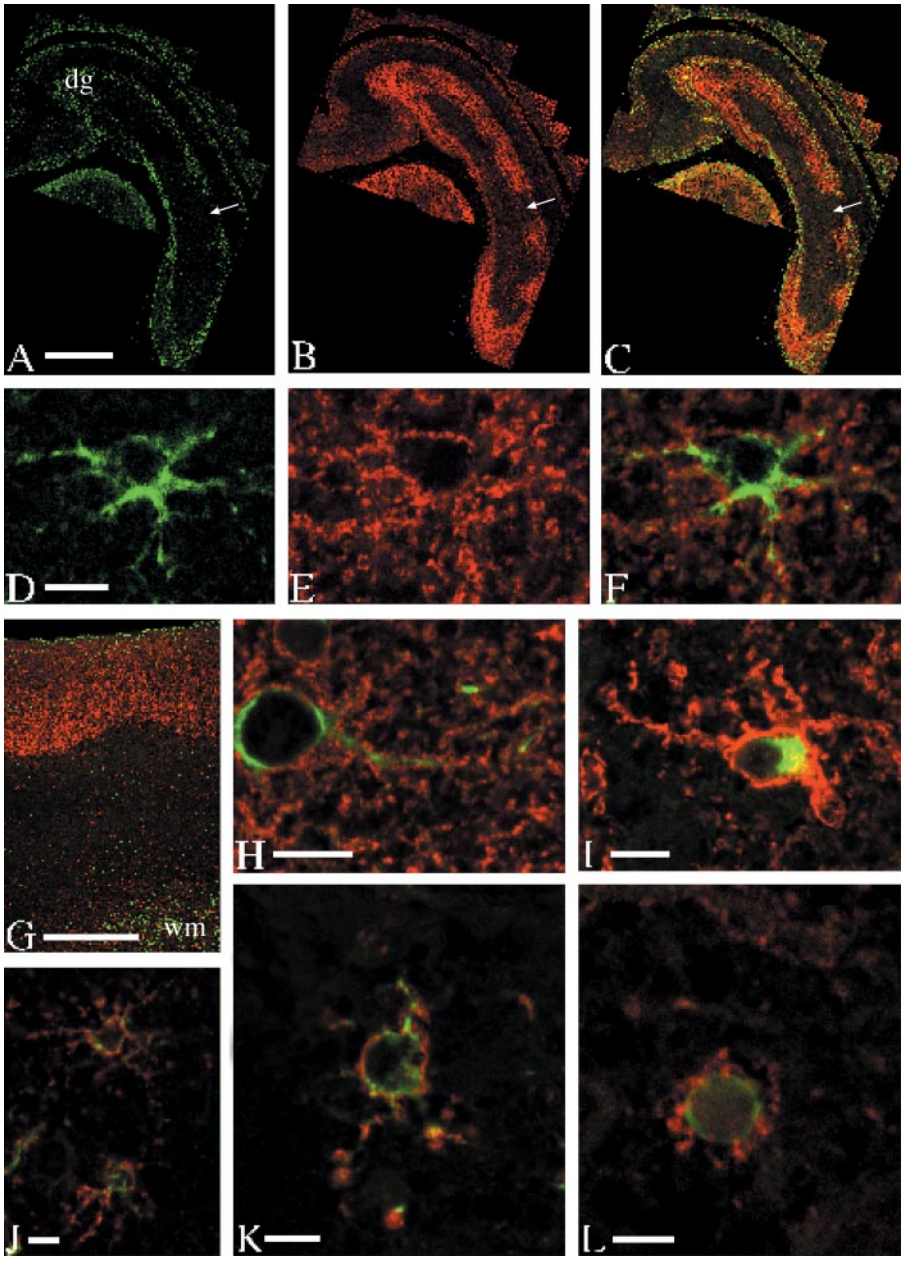

FIGURE 8. **Dual immunofluorescence labeling in control and hypoxic pig brains for GFAP (*green*) and GLAST (*red*).** *A–C*, a montage of confocal images from the hypoxic pig hippocampus labeled for GFAP (*A*) and GLAST (*B*). The merged image (*C*) illustrates a tight spatial association between GFAP and GLAST in the hippocampus after hypoxia. *Arrows* indicate an area where both GFAP and GLAST are lost. *D–F*, control pig cortical gray matter astrocyte. GFAP (*D*) was expressed in the core of the astrocyte, and GLAST (*E*) was co-expressed in the plasma membrane (*F*). *G*, hypoxic cortex showed tight spatial association between GFAP and GLAST. *H*, astrocyte from the dentate region of hypoxic pig brain. GFAP and GLAST labeling extended along the length of its processes. *I–L*, astrocytes from hypoxic pig tissue showed astrocytes in brain regions damaged by hypoxia. These astrocytes showed abnormal morphology, with short, distorted processes and reduced expression of GFAP and GLAST (*I–K*). In many cells (*L*), GFAP labeling was restricted to the cell body and very little expression of GLAST was evident in remnant processes. *dg*, dentate gyrus; *wm*, white matter. *Scale bars*, *A–C*, 250 μm; *D–F* and *H–L*, 5 μm; *G*, 100 μm.

where GFAP was also up-regulated (Fig. 8*G*). In these cortical areas and other areas such as the dentate gyrus of the hippocampus, astrocytes appeared to have normal morphology and showed co-association of GFAP and GLAST in their distal processes (Fig. 8*H*). In areas where severe cellular damage was evident, astrocytes exhibited an abnormal morphology, with expression of GFAP (and concomitant expression of GLAST) restricted to the proximal processes and soma of the astrocyte (Fig. 8, *I–L*). Some astrocyte processes appeared completely retracted, with GFAP only expressed in the soma and GLAST expression restricted to around the cell body (Fig. 8*L*).

DISCUSSION

In this study we have identified a novel association between GFAP and GLAST that appears to result in the anchoring of GLAST in the plasma membranes of astrocytes and enhancement of GLAST-mediated transport. This is significant because a well defined functional role for GFAP has not previously been identified.

Previous studies have noted that glutamate transporters are targeted or anchored in specific cellular compartments of astrocytes (20). This targeting or anchoring process is significant because the localization of GLAST will influence its capacity to regulate extracellular glutamate; however, to date, there has been limited evidence as to how this anchoring or targeting might be achieved.

A clue as to the possible mechanism by which GFAP might serve to anchor GLAST is provided by earlier studies. An *in vivo* association was previously shown between GLAST, NHERF1, and ezrin (17, 21). In this study we have extended these findings; our D-aspartate uptake and co-immunoprecipitation experiments in cultured cells have highlighted the importance of the C-terminal PDZ binding motif (ETKM) of GLAST in both functional transport and in mediating the interaction with GFAP. Our results also suggest that the interaction between GFAP and GLAST is indirect but dependent upon the presence of NHERF1.

We further demonstrate a molecular association between GFAP and GLAST in rat and pig brain. We propose that GFAP stabilizes the process of the astrocyte and allows the retention of GLAST in the plasma membrane via a series of intermediate, linking proteins, including NHERF1 and ezrin (Fig. 9).

In support of this model, it has been shown that each of these proteins is expressed in astrocytes. Moreover, Derouiche and

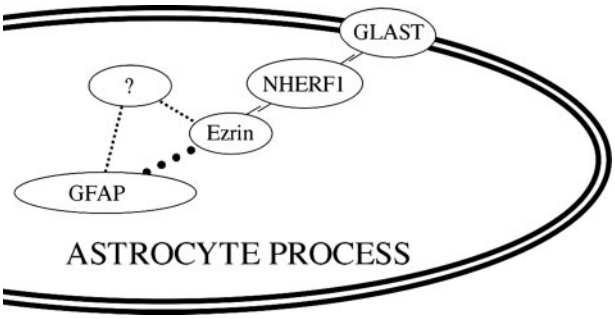

FIGURE 9. **Diagram illustrating proposed associations between GFAP and GLAST in astrocytes.** Immunoprecipitation results indicated that these four proteins, GLAST, NHERF1, ezrin, and GFAP form part or all of a functional complex. The associations between ezrin, NHERF1, and GLAST are probably direct, as indicated. The interaction between ezrin and GFAP may be direct (depicted by the *dotted line*) or may potentially involve another, as yet undefined, accessory protein/s (as depicted by the *dashed lines*).

Frotscher (22) have shown that the GFAP cytoskeleton is intimately associated with actin-associated ezrin, radixin, and moesin (ERM) proteins and that immunoreactivity for ERM proteins extends from the GFAP cytoskeleton out to the plasma membranes of the astrocytes. Whether the linkage between GFAP and ezrin is direct or via one or more additional linking proteins remains to be determined. We note in our Coomassie blue-stained gels that there are at least ten proteins that might provide additional linkages in our model.

Our model would suggest that any change in GFAP expression or localization would influence glutamate homeostasis. This hypothesis is supported by our D-aspartate transport results and the recent observation that GFAP knock-out mice exhibit reduced glutamate clearance and may be more sensitive to hypoxia than normal mice (4). Given the preceding evidence, the model we propose indicates that the association between GFAP and GLAST will be important under normal physiological conditions because any modulation of the localization of GLAST will influence its capacity to regulate extracellular glutamate.

The loss of GLAST from some brain regions in response to an episode of hypoxia (and retention in other brain regions) accords with other studies (15, 23–30). The novel facet of this study is the observation that the redistribution of GLAST is associated with redistribution of GFAP in the same cells, an observation that is compatible with our proposed model.

We have observed that in response to hypoxia, astrocytes in damaged brain regions exhibit an abnormal morphology, characterized by the presence of very short processes and a redistribution of immunoreactivity for both GFAP and GLAST from the processes into the somata. Conversely, in undamaged brain regions we observe an increase in the expression of GFAP that coincides with the retention of GLAST protein in these astrocyte processes. These observations accord with the proposed model.

Because GFAP is thought to stabilize astrocyte processes, loss of GFAP has consequences not only for glutamate homeostasis but also for astrocyte morphology. Our view, that homeostasis of glutamate and astrocyte morphology are intimately linked with GFAP expression, is of potential relevance to many disease states besides hypoxia. GFAP is up-regulated in diseases such as epilepsy and amyotrophic lateral sclerosis where abnormal excitation may be implicated in the pathophysiology of the disease (31–35). However, at the individual cell level, there are no current data as to whether there are correlated changes in the expression of GLAST.

Collectively, our data and data from the literature support the view that the GFAP cytoskeleton of the astrocyte may be a key component in normal astrocyte function and that anchoring proteins such as GLAST to the cytoskeleton may be an important element in glutamate homeostasis. Accordingly, developing therapies that protect or promote the interaction between these proteins may be useful neuro-protective strategies.

Acknowledgments—We thank Dr. Chris Yun for the generous gift of the NHERF1 antibody. We thank Dr. Michael Brenner for the generous gift of the GFAP plasmid and Dr. Didier Trono for the generous gifts of the psPAX2 and pMD2G plasmids.

REFERENCES

1. Pekny, M., and Pekna, M. (2004) *J. Pathol.* **204,** 428–437
2. Eng, L. F., Ghirnikar, R. S., and Lee, Y. L. (2000) *Neurochem. Res.* **25,** 1439–1451
3. Messing, A., and Brenner, M. (2003) *Glia* **43,** 87–90
4. Hughes, E. G., Maguire, J. L., McMinn, M. T., Scholz, R. E., and Sutherland, M. L. (2004) *Brain Res. Mol. Brain Res.* **124,** 114–123
5. Danbolt, N. C., Storm-Mathisen, J., and Kanner, B. I. (1992) *Neuroscience* **151,** 295–310
6. Kanner, B. I., and Sharon, I. (1978) *FEBS Lett.* **94,** 245–248
7. Zerangue, N., and Kavanaugh, M. P. (1996) *Nature* **383,** 634–637
8. Choi, D. W. (1990) *J. Neurosci.* **10,** 2493–2501
9. Choi, D. W., and Rothman, S. M. (1990) *Annu. Rev. Neurosci.* **13,** 171–182
10. Jensen, F. E. (1999) *Epilepsia* **40,** Suppl. 1, S51-S58
11. Jensen, F. E., Applegate, C. D., Holtzman, D., Belin, T. R., and Burchfiel, J. L. (1991) *Ann. Neurol.* **29,** 629–637
12. Mishra, O. P., and Delivoria-Papadopoulos, M. (1999) *Brain Res. Bull.* **48,** 233–238
13. Johnston, M. V., Trescher, W. H., Ishida, A., and Nakajima, W. (2001) *Pediatr. Res.* **49,** 735–741
14. Johnston, M. V., Nakajima, W., and Hagberg, H. (2002) *Neuroscientist* **8,** 212–220
15. Pow, D. V., Naidoo, T., Lingwood, B. E., Healy, G. N., Williams, S. M., Sullivan, R. K. P., O'Driscoll, S., and Colditz, P. B. (2004) *Dev. Brain Res.* **153,** 1–11
16. Williams, S. M., Sullivan, R. K. P., Scott, H. L., Finkelstein, D. I., Colditz, P. B., Lingwood, B. E., Dodd, P. R., and Pow, D. V. (2005) *Glia* **49,** 520–541
17. Lee, A., Rayfield, A., Hryciw, D., Ma, T. A., Pow, D. V., Broer, S., Yun, C., and Poronnik, P. (2007) *Glia* **55,** 119–129
18. Bjorkman, S. T., Foster, K. A., O'Driscoll, S. M., Healy, G. N., Lingwood, B. E., Burke, C., and Colditz, P. B. (2006) *Brain Res.* **1100,** 110–117
19. Haugeto, O., Ullensvang, K., Levy, L. M., Chaudhry, F. A., Honore, T., Nielsen, M., Lehre, K. P., and Danbolt, N. C. (1996) *J. Biol. Chem.* **44,** 27715–27722
20. Sullivan, R. K. P., Rauen, T., Fischer, F., Wiessner, M., Grewer, C., Bicho, A., and Pow, D. V. (1994) *Glia* **45,** 155–169
21. Yun, C. H., Lamprecht, G., Forster, D. V., and Sidor, A. (1998) *J. Biol. Chem.* **40,** 25856–25863
22. Derouiche, A., and Frotscher, M. (2001) *Glia* **36,** 330–341
23. Bruhn, T., Levy, L. M., Nielsen, M., Christensen, T., Johansen, F. F., and Diemer, N. H. (2000) *Neurochem. Int.* **37,** 277–285
24. Fukamachi, S., Furuta, A., Ikeda, T., Ikenoue, T., Kaneoka, T., Rothstein, J. D., and Iwaki, T. (2001) *Brain Res. Dev. Brain Res.* **132,** 131–139
25. Martin, L. J., Brambrink, A. M., Lehmann, C., Portera-Cailliau, C., Koehler, R., Rothstein, J., and Traystman, R. J. (1997)) *Ann. Neurol.* **42,** 335–348

26. Rao, V. L., Baskaya, M. K., Dogan, A., Rothstein, J. D., and Dempsey, R. J. (1998) *J. Neurochem.* **70,** 2020–2027
27. Rao, V. L., Bowen, K. K., and Dempsey, R. (2001) *Neurochem. Res.* **26,** 497–502
28. Tao, F., Lu, S. D., Zhang, L. M., Huang, Y. L., and Sun, F. Y. (2001) *Neuroscience* **102,** 503–513
29. Torp, R., Lekieffre, D., Levy, L. M., Haug, F. M., Danbolt, N. C., Meldrum, B. S., and Ottersen, O. P. (1995) *Exp. Brain Res.* **103,** 51–58
30. Yi, J. H., Pow, D. V., and Hazell, A. S. (2004) *Glia* **49,** 121–133
31. Chengyun, D., Guoming, L., Elia, M., Catania, M. V., and Qunyuan, X. (2006) *Neurol. Sci.* **27,** 245–251
32. Vessal, M., Dugani, C. B., Solomon, D. A., McIntyre Burnham, W., and Ivy, G. O. (2005) *Brain Res.* **1044,** 190–196
33. Kushner, P. D., Stephenson, D. T., and Wright, S. (1991) *J. Neuropathol. Exp. Neurol.* **50,** 263–277
34. Nagy, D., Kato, T., and Kushner, P. D. (1994) *J. Neurosci. Res.* **38,** 336–347
35. Tessler, S., Danbolt, N. C., Faull, R. L., Strom-Mathisen, J., and Emson, P. C. (1999) *Neuroscience* **88,** 1083–1091

Membrane Transport, Structure, Function, and Biogenesis:

Cytoskeletal Anchoring of GLAST Determines Susceptibility to Brain Damage: AN IDENTIFIED ROLE FOR GFAP

Susan M. Sullivan, Aven Lee, S. Tracey Björkman, Stephanie M. Miller, Robert K. P. Sullivan, Philip Poronnik, Paul B. Colditz and David V. Pow

J. Biol. Chem. 2007, 282:29414-29423.
doi: 10.1074/jbc.M704152200 originally published online August 6, 2007